Perspective

Carbon Future

What insights can we learn from dimensionally stable anodes (DSAs)?

Xianbiao Fu

Department of Physics, Technical University of Denmark, Kongens Lyngby, Denmark

Cite This: *Carbon Future* **2024**, *1*, 9200027

Read Online

ABSTRACT: The chlor-alkali process is a cornerstone of the chemical industry. The development of dimensionally stable anodes (DSAs) has revolutionized the chlor-alkali industry by significantly improving the efficiency and stability of chlorine production. Originally designed to address the limitations of graphite and platinum anodes, DSAs are composed of titanium substrates coated with mixed metal oxides, such as ruthenium and titanium oxides, which offer superior catalytic stability and corrosion resistance. This perspective explores the historical evolution of DSAs, their intrinsic properties, and performance benefits, emphasizing the pivotal role of the gas-bubble effect in reducing cell voltage and subsequently reducing energy consumption. The development of DSA provides a clear example of how optimizing catalyst composition, refining the preparation process, and managing gas bubble dynamics can significantly enhance the stability and efficiency of industrial electrochemical systems. These critical insights can extend to other important electrochemical processes, such as water electrolysis and fuel cells. This perspective identifies the need for standardized stability testing protocols to enhance the evaluation of catalyst durability.

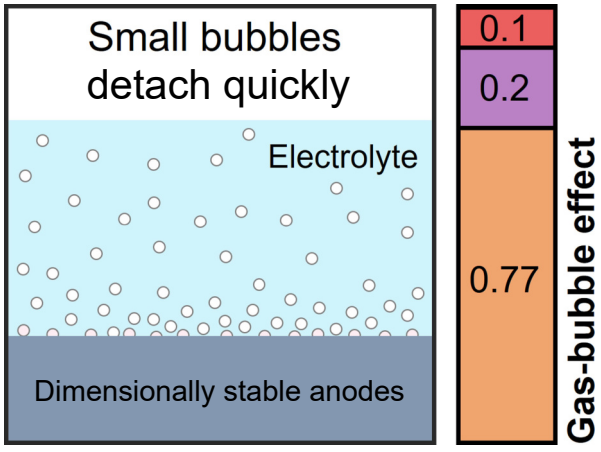

KEYWORDS: dimensionally stable anodes, gas-bubble effect, chlor-alkali electrolysis, stability assessment, mixed metal oxide

Chlor-alkali electrolysis is one of the most mature and widely used industrial electrochemical processes, responsible for producing chlorine gas (Cl_2), sodium hydroxide (NaOH), and hydrogen gas (H_2) via electrolysis of sodium chloride (NaCl) solution (i.e., brine)[1,2]. These products are vital in various industries such as chemical manufacturing, water treatment, paper production, and the production of plastics like polyvinyl chloride (PVC). Chlorine production exceeds 90 million metric tons annually, and with NaOH produced in equimolar quantities surpassing 100 million metric tons, chlor-alkali technology ranks among the largest chemical sectors worldwide, following only sulfuric acid and ethylene production[3,4]. Three primary techniques are employed in the electrolytic production of chlorine: the diaphragm cell (Griesheim cell, developed in 1885), the mercury cell (Castner–Kellner cell, introduced in 1892), and the membrane cell technique (1970)[2]. The energy consumption per ton of Cl_2 varies among these methods, with mercury cells requiring between 3000 and 4400 kWh, diaphragm cells consuming 2600 to 3100 kWh, and membrane cells utilizing 2000 to 3000 kWh[2]. Notably, the energy consumption figures mentioned above greatly benefit from the significant contributions of dimensionally stable anodes (DSAs). Chlor-alkali electrolysis accounts for approximately 10% of global electricity consumption. Therefore, the chlor-alkali industry is increasingly focusing on innovative technologies to reduce the energy cost of Cl_2 production. Significant advancements in chlor-alkali technology include the invention of DSA and the design of membrane cells, both of which have proven effective in reducing the energy required per ton of Cl_2 produced[5]. In the membrane cell technique for chlor-alkali electrolysis, the anode and cathode compartments are separated by an ion-conducting membrane (Fig. 1). Simultaneously, sodium ions (Na^+) migrate through the membrane into the cathode compartment, where they combine with hydroxide ions (OH^-) to produce NaOH. The ion-conducting membrane plays a crucial role in this technique by allowing only specific ions, such as sodium ions, to pass through while preventing the mixing of chlorine gas and the caustic soda solution, which enhances product purity and efficiency[2]. The invention of DSA anodes has significantly impacted the chlor-alkali industry by reducing energy consumption and enhancing process stability,

Received: October 12, 2024; **Revised:** December 8, 2024
Accepted: December 19, 2024

Address correspondence to Xianbiao Fu, xiafu@dtu.dk

https://doi.org/10.26599/CF.2024.9200027

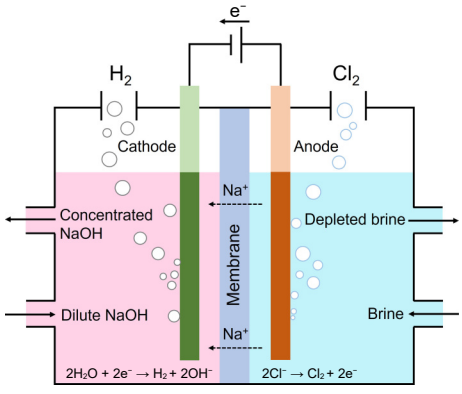

Fig. 1. Schematic of the chlor-alkali electrolyzer (membrane cell).

regardless of the chlorine production technology utilized[6, 7]. The invention of DSA has transformed the chlor-alkali process and offers valuable lessons for emerging technologies, including water splitting for H_2 production, CO_2 reduction, and N_2 reduction for ammonia synthesis[8–10]. By analyzing the key features and advantages of DSA, we can draw insights that may enhance the durability and industrial viability of these technologies.

Initially, platinum, magnetite, and carbon were used as anode materials for Cl_2 production, but each had notable limitations[7]. Platinum, though effective, proved too expensive, insufficiently resistant to chlorine, and energy-intensive. Magnetite faced issues such as poor machinability, fragility, and low conductivity—only 5% of graphite's conductivity—limiting its maximum anode current density to 0.4 A·cm^{-2}. This led to the widespread adoption of graphite anodes from the early 1900s until the late 1960s[2]. However, graphite anodes presented several significant challenges. Their short lifespan (6–24 months) required frequent replacement, and they consumed several pounds of graphite per ton of Cl_2 produced. Additionally, they contaminated the product stream with chlorinated hydrocarbons, which could clog pumps and pipes[6, 7]. Graphite particles also had a detrimental impact on diaphragm performance, leading to stray currents and energy losses. Furthermore, their erosion resulted in an increased anode–cathode gap over time, leading to higher cell voltage and greater energy consumption[6, 7]. These limitations prompted the search for more efficient and durable anode materials, as ensuring stable operation and minimizing contamination became increasingly important in industrial processes.

In 1956, while attempting to prepare ferrotitanate using iron and titanium (Ti) anodes, Beer discovered that Ti became inert in chloride-containing electrolytes due to the formation of an oxide layer, which blocked current flow[6, 7]. After testing other electrolytes with similar outcomes, he realized that Ti could be an ideal substrate for anodes in chlorine-alkali electrolysis, provided it was coated with a conductive, electrocatalytically active, and chemically inert material that would maintain conductivity under anodic conditions. In the early 1960s, Henri Bernard Beer first tested platinum-coated Ti anodes for chlorine production but failed due to high platinum wear rates, premature coating losses, and passivation during operation, especially in mercury cells[6, 7, 11]. The excessive overpotential also led to high energy consumption, making them no better than graphite anodes. It was also discovered that proper pretreatment of the Ti was crucial for applying an active layer with good adhesion. Therefore, the Ti was thoroughly degreased chemically and electrolytically, and all surface contaminants like oxides were removed to enhance the coating's adhesive properties. In 1967, Henri Bernard Beer solved these problems by developing a new generation of anodes using ruthenium oxide (RuO_2) stabilized with titanium oxide (TiO_2) coatings on titanium substrates (RuO_2-TiO_2/Ti) via a thermal decomposition technique (Figs. 2a and 2b)[12, 13]. The RuO_2-TiO_2/Ti anodes presented extraordinary electrocatalytic activity and stability for Cl_2 production. This type of DSA is now generally used in chlorine-alkali electrolysis across mercury, diaphragm, and membrane cells. The invention of DSA primarily involves Ti substrates coated with mixed metal oxides, such as ruthenium and iridium. Later studies introduced a conductive metal layer, such as Pt or Ir, plated onto the Ti as an intermediate layer before applying the active coating to avoid the influence of the TiO_x passivation layer on the Ti surface. The RuO_2-TiO_2/Ti anodes demonstrated a long lifespan, lasting approximately 8 years in diaphragm cells and 2 years in mercury cells[1]. The lifetime of RuO_2-TiO_2-SnO_2/Ti anodes was at least 12 years in diaphragm cells[2]. DSAs offer superior chemical stability against corrosion in harsh chlorine and alkaline environments, longer lifespans reducing the need for replacements, and lower overpotentials for chlorine evolution that decrease energy consumption. The invention of DSA is regarded as one of the most significant technological breakthroughs in electrochemistry over the past 70 years[14].

The technological innovation of DSA is driven by industrial demand rather than scientific exploration (i.e., from laboratory research to industrial application). While the industry was actively testing the performance of DSA, the electrochemistry community had little understanding of conductive oxide electrodes[14]. In 1971, Trasatti conducted pioneering research on the fundamental properties and electrochemical behavior of RuO_2[15]. Despite DSAs already being in industrial use by the 1970s, it indeed took years of research to fully understand the underlying mechanisms that contributed to their exceptional performance. In 2000, Trasatti attempted to further understand the success of DSA by analyzing technical data on the overpotential contributions of their different components[14]. Those technical data were obtained from De Nora mercury cells and were originally reported by O. De Nora in 1970[16]. As shown in Fig. 2c, the slope of the relationship between current density and cell voltage is notably steeper with graphite electrodes compared to DSA, indicating a higher cell voltage for a given current density. In De Nora mercury cells, the energy consumption for producing one ton of Cl_2 with graphite anodes is 3910 kWh, whereas using DSA anodes reduces it to 3040 kWh per ton[16]. Given the large scale of Cl_2 production, the energy savings achieved with DSA anodes are substantial. The cell voltages are 4.97 V with graphite anodes and 3.9 V with DSA at a current density of 1 A·cm^{-2}, respectively (Fig. 2d). This means that replacing the graphite anode with a DSA results in a voltage reduction of 1.07 V. This often leads to the simplistic conclusion that DSA's superior performance is solely due to its batter electrocatalytic activity compared to graphite anodes. However, this is not the case. Further analysis reveals that the voltage reduction directly attributable to DSA's electrocatalytic activity is only about 0.1 V (Fig. 2d). Approximate 0.2 V of the voltage reduction can be attributed to the lower ohmic drop resulting from the shorter distance of anode-cathode (2 mm). The most significant factor in the 0.77 V reduction is due to the improved mass transport properties and the reduction of gas-bubble accumulation, commonly known as the gas-bubble effect, on the surface of the DSA (Fig. 2d)[4, 14, 16]. These characteristics minimize the resistive losses that are often

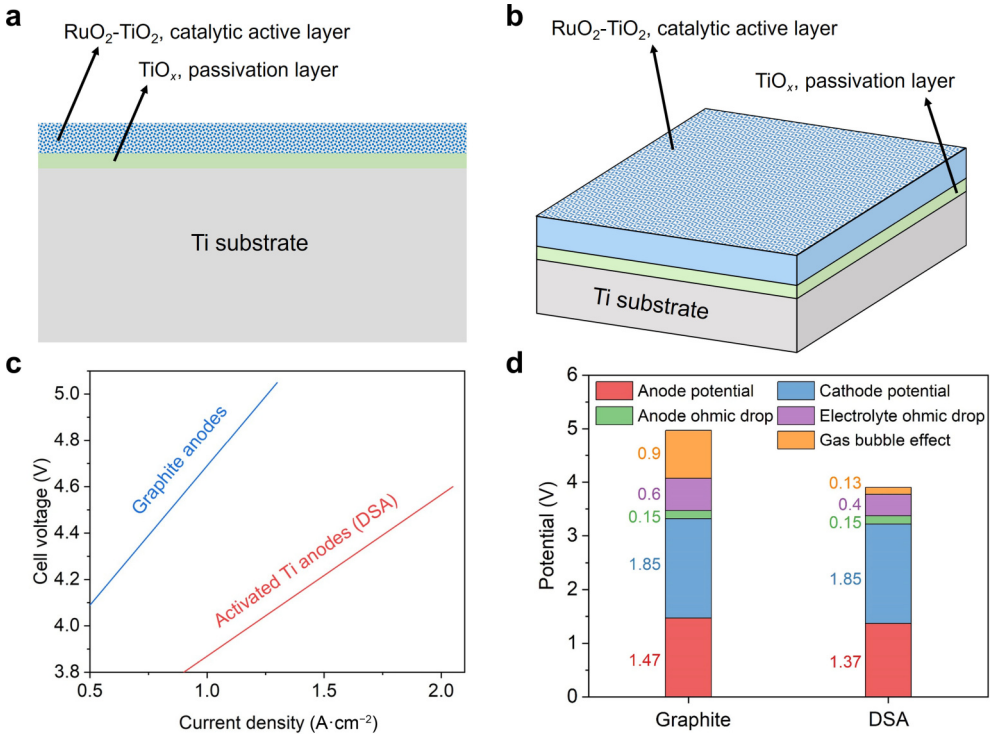

Fig. 2. Impact of DSA on efficiency of chlor-alkali electrolysis. **a**, Side view of DSA. **b**, Top view of DSA. **c**, The cell voltage difference versus current density for De Nora mercury cells varies depending on the type of anode used (graphite and DSA). NaCl concentration: 310 g·L^{-1}. Temperature: 60 °C. **d**, Comparison of the voltage components of de Nora mercury cells at a current density of 1 A·cm^{-2} with graphite or DSA anodes. The electrolyte ohmic drops were 0.6 and 0.4 V for anode-cathode distances of 3 and 2 mm, respectively[16].

encountered with graphite anodes, where gas bubbles tend to block active sites and hinder efficient ion transport. Additionally, the superior chemical stability and corrosion resistance of DSA under harsh operating conditions contribute to their long-term stability, further reducing the need for frequent electrode replacements and maintenance. The success of DSAs can be attributed to their optimized surface morphology, which mitigates the gas-bubble effect and enhances mass transport, along with their exceptional chemical stability and corrosion resistance under harsh conditions. These findings underscore the importance of addressing mass transport limitations and ensuring long-term stability in the design of electrodes for other electrocatalytic reactions, where similar considerations can significantly improve performance and efficiency.

Given the significant impact of the gas-bubble effect, it will be discussed in more detail, particularly in electrochemical reactions involving gas evolution under industrial conditions[17–21]. Gas bubbles forming at the electrode surface typically undergo nucleation, growth, and eventual detachment (Fig. 3a)[19]. The longer a bubble grows and remains on the electrode surface, the more it hinders mass transport by blocking the active sites of the electrode, thereby reducing the effective surface area for the electrochemical reaction and increasing the local overpotential[19]. Prolonged bubble residence also creates concentration gradients that intensify the mass transport limitations, making it increasingly difficult for reactants to reach the electrode surface. This obstruction not only hinders the diffusion of reactants but also impedes the removal of reaction products, leading to a significant drop in efficiency. Therefore, an ideal electrode for gas evolution should minimize the bubble growth and residence time as much as possible. The size and frequency of bubble departure from the electrode surface have a significant effect on the overpotential in electrochemical systems, as faster and smaller bubble departures help maintain efficient mass transport and lower the local overpotential (Fig. 3b)[22]. Due to the nano/microstructure and surface morphology, along with the intrinsic properties of their active coatings, DSA anodes are more effective than graphite anodes at minimizing bubble adhesion and promoting faster gas bubble detachment. Constructing nano/microstructures on graphite anodes through surface engineering does not enable them to match the performance of Ti-based DSA anodes. This is because graphite is vulnerable to oxidation and degradation of surface structures, and its weaker mechanical properties make it prone to fragmentation, leading to potential system clogging and reduced long-term stability. Recent advancements have focused on modifying electrode surfaces, engineering nano/micro-scale architectures, and adjusting electrolyte compositions to alleviate the negative impact of gas bubbles[17–22]. By fine-tuning the surface wettability, it is possible to reduce bubble adhesion and promote more efficient bubble detachment. For example, applying hydrophobic coatings can decrease the surface energy, facilitating the release of gas bubbles and minimizing their residence time on the electrode[22]. Studies have highlighted the impact of electrolyte type on bubble behavior, where the anions present in solution play a critical role in influencing the detachment dynamics of gas bubbles from the electrode surface[23]. Koper and colleagues revealed that different anions follow the Hofmeister series, affecting the detachment size and frequency of hydrogen gas bubbles. Anions like those in sulfuric acid led to larger bubbles that detach less frequently, while those in perchloric acid result in smaller bubbles that detach more frequently due to the forces at play, such as Marangoni flows[23,24].

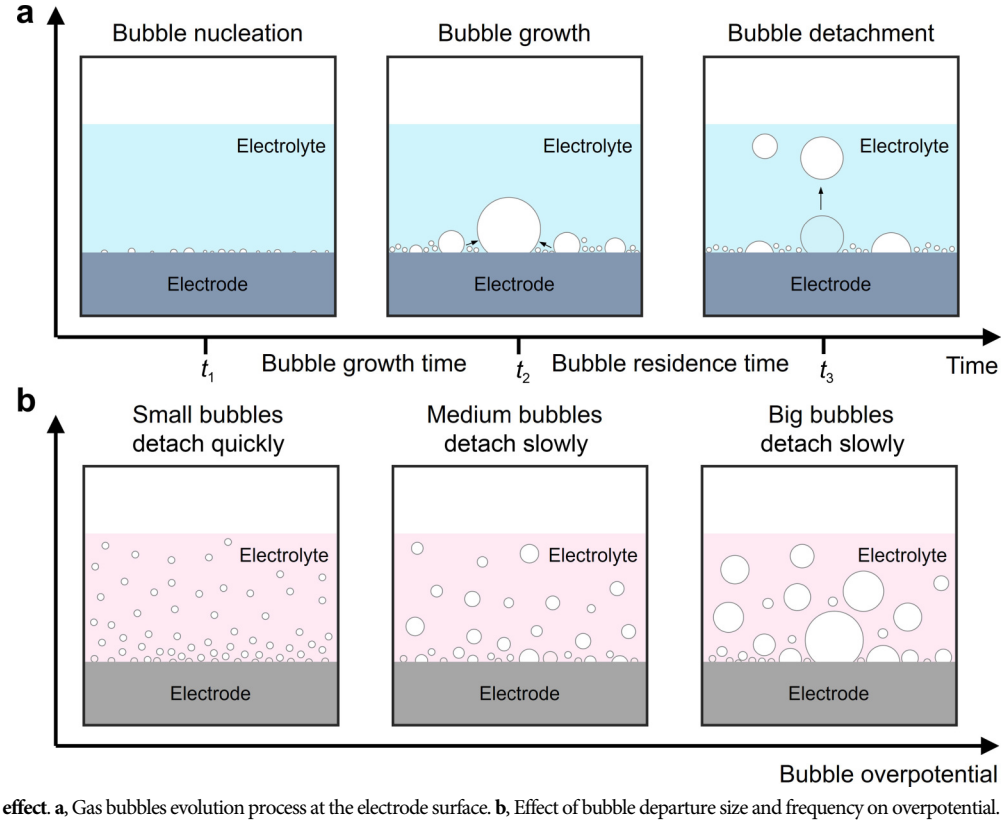

Fig. 3. Gas-bubble effect. **a**, Gas bubbles evolution process at the electrode surface. **b**, Effect of bubble departure size and frequency on overpotential.

Previous studies focused on bubble behavior at the micrometer scale using high-speed cameras. The behavior of bubbles during gas evolution reactions at the nanoscale, however, remains largely unexplored[18]. Several critical questions remain unanswered: (1) How do the composition and atomic-scale structure of the electrode influence bubble nucleation and detachment dynamics? (2) Is the nucleation rate of gas bubbles primarily governed by the intrinsic properties of the electrode surface, such as its chemical composition and electronic structure, or is it more strongly influenced by the micro/nanostructural features of the electrode? (3) In the membrane electrode assembly (MEA) electrolyzer and flow cell, how do gas bubbles affect the ion-conductive polymer electrolyte/electrode interface and the triple-phase boundaries (i.e., electrode–electrolyte–gas interfaces) under industrial operating conditions? Addressing these questions is crucial for understanding the fundamental mechanisms of gas evolution at the nanoscale, which may differ significantly from behaviors observed at larger scales. At the nanoscale, factors such as localized surface energy variations, defect sites, and the distribution of active sites could play a more prominent role in influencing bubble nucleation and growth. Techniques such as *operando* synchrotron-based X-ray imaging, neutron scattering, and *in situ* electron microscopes could provide insights into how gas bubbles form, grow, and interact with the electrode and electrolyte at both the nanoscale and in practical electrolyzers. Additionally, integrating high-resolution imaging with electrochemical measurements could allow for simultaneous monitoring of bubble dynamics and reaction kinetics, offering a comprehensive understanding of the impact of bubbles on electrochemical performance. When assessing the electrocatalytic activity of electrodes, it is crucial to minimize the impact of gas bubbles to obtain accurate and reliable results. Increasing the rotation speed of a rotating disk electrode (RDE) or using forced convection helps remove bubbles and reduce mass transport limitations. Additionally, optimizing electrode orientation and surface design can facilitate bubble detachment and prevent active site blockage.

While advancements in electrocatalyst activity often take center stage, the remarkable success of DSA highlights the equally crucial role of electrocatalyst stability in electrocatalytic applications. Unfortunately, research on catalyst stability is frequently overshadowed by the pursuit of higher activity, leading to a gap in developing truly durable electrocatalysts[25]. This oversight can result in electrocatalysts that, despite their initial efficiency, fail to perform effectively over time. Therefore, a balanced focus on both activity and stability is essential for the sustainable advancement of electrocatalysis technology. The development of DSA and acidic oxygen evolution reaction (OER) catalysts has revealed that the primary factor influencing catalyst dissolution is the intrinsic properties of their composition[14, 26]. Secondary factors include the preparation methods, surface structure/morphology, and test environment. For instance, IrO_2 stands out as the most stable known acidic OER catalyst, primarily due to its robust chemical composition and structural stability under acidic conditions[26]. Despite RuO_2-TiO_2/Ti anode being widely used in the chlorine-alkali industry, they are not stable for oxygen evolution in acidic environments. RuO_2 is at least two orders of magnitude less stable than IrO_2 under similar acidic OER conditions[26]. Under anodic potential in acidic media, RuO_2 undergoes dissolution and oxidation to soluble RuO_4, leading to gradual loss of the active material. It should be noted that the RuO_2-TiO_2/Ti anode contains Ti-doped RuO_2 and RuO_2-TiO_2 mixed oxides, though their exact proportions remain unconfirmed. Although Ti-doping or the presence of TiO_2 can improve stability to some extent, it cannot completely inhibit the formation and dissolution of RuO_4. Building

on the success of DSA, researchers have been continually inspired to explore more stable anode catalyst compositions for various electrochemical reactions, including acidic OER. Consequently, numerous DSA anode catalysts have been developed by mixing different oxides and incorporating metal dopants (Table 1)[11–13, 27–48]. This strategy leverages both the composition effect and synergy effect among the constituent elements, significantly enhancing the electrochemical stability and activity of the anode. Research on these DSA anodes provides valuable insights for the development of other stable anode catalysts, such as acidic OER catalysts. However, most DSA catalysts have not been thoroughly characterized before and after stability tests, and their metal dissolution rates have rarely been assessed. Notably, mass-selected $Ir_{0.1}Ta_{0.9}O_{2.45}$ clusters have been shown to exhibit high catalytic activity and stability for acidic OER, confirming that mixed metal oxides on the atomic scale can form unique iridium coordination environments that serve as highly active sites for OER[49]. Additionally, exploring the atomic-scale interactions in mixed metal oxides may unveil new pathways to tailor active sites and improve activity and stability in acidic OER and beyond. Future detailed research could potentially unlock new insights and stability mechanisms related to DSA catalysts at atomic scale, which could provide new opportunities for DSA in various electrocatalytic applications.

Ti was commonly used as a substrate in DSA. The substrate significantly influences catalyst stability by affecting mechanical integrity, electron conductivity, and corrosion resistance. For instance, carbon-based substrates are prone to oxidation, while metal substrates like titanium or nickel offer greater durability under harsh conditions. Strong catalyst–substrate interactions and interfacial stability are crucial for maintaining long-term performance and minimizing degradation. Exploring alternatives to Ti substrates for potential systems is a relevant consideration, given Ti's relatively high cost. Several metals have been investigated as

Table 1 Summary of DSA catalysts performance and test conditions

Year	Composition	T (°C)	j (A·cm^{-2})	Electrolyte	Stability (h)	Ref.
1961	Ir/Ti	NA	NA	NA	NA	11
1967	RuO_2-TiO_2/Ti	80	1	5.8 M NaCl	NA	12
1977	RuO_2-TiO_2/Ti	25	0.5	0.25 M H_2SO_4	3.3	27
1979	RuO_2-TiO_2/Ti	40	2	2 M $HClO_4$ + 2 M NaCl	260	28
1981	IrO_x/Ti	25	NA	NA	NA	29
1981	RuO_x/Ti	25	NA	NA	NA	29
1981	$IrRuO_x$/Ti	25	NA	NA	NA	29
1981	$RuTa_{0.5}Ir_{0.5}O_x$/Ti	25	NA	NA	NA	29
1982	RuO_2/Ru-Ir/Pd/Ti	70	0.05	0.5 M $NiSO_4$ + 0.4 M H_2SO_4	20,266	30
1991	IrO_2-Ta_2O_5/Ti	80	0.75	3.7 M H_2SO_4	220	31
1991	IrO_2-ZrO_2/Ti	80	0.75	3.7 M H_2SO_4	NA	31
1991	IrO_2-TiO_2/Ti	80	0.75	3.7 M H_2SO_4	NA	31
1994	IrO_2-Ta_2O_5/Ti	25	2	0.5 M H_2SO_4	7049	32
1996	$Ru_{0.3}Ti_{0.7-x}Ce_xO_2$/Ti	25	NA	1 M $HClO_4$	NA	33
1997	SnO_2-Sb_2O_5/Ti	25	0.1	1 M H_2SO_4	12	34
1997	SnO_2-Sb_2O_5/IrO_2/Ti	25	0.1	1 M H_2SO_4	900	34
1998	$Ir_{0.3}Ti_{0.7}O_2$/Ti	32	0.4	1 M $HClO_4$	510	35
2000	IrO_2-Nb_2O_5/Ti	50	0.8	1 M $HClO_4$	330	36
2001	IrO_x-Sb_2O_5-SnO_2/Ti	35	1	3 M H_2SO_4	1600	37
2002	IrO_2-Ta_2O_5/Ti	50	2	0.5 M H_2SO_4	780	38
2002	$Ru_xMn_{1-x}O_2$/Ti	25	1	0.5 M H_2SO_4	20	39
2003	IrO_2-Ta_2O_5/Ti	30	2	1 M H_2SO_4	482	40
2005	RuO_2-Sb_2O_5-SnO_2/Ti	25	0.5	3 M H_2SO_4	307	41
2006	IrO_2-Ta_2O_5/Ti	40	2	0.5 M H_2SO_4	630	42
2010	RuO_2-IrO_2-TiO_2/Ti	25	2	0.5 M NaCl	260	43
2011	RuO_2-Sb_2O_5-SnO_2/Ti	35	1	0.5 M NaCl	266	44
2011	$Ru_{0.3}Ti_{0.7}O_2$/Ti	25	0.6	0.5 M NaCl	18	45
2011	$Ru_{0.3}Ti_{0.4}Ir_{0.3}O_2$/Ti	25	0.6	0.5 M NaCl	30	45
2012	RuO_2-IrO_2-SnO_2-Sb_2O_5/Ti	25	2	0.5 M NaCl	658	46
2013	$Ru_{0.25}Ir_{0.25}Ti_{0.5}O_2$/Ti	25	2	1 M H_2SO_4	293	47
2013	$Ru_{0.25}Ir_{0.25}Ti_{0.5}O_2$/Ti	25	2	0.5 M NaCl	104	47
2015	IrO_2-Ta_2O_5/Ti	60	4	0.5 M H_2SO_4	916	48

possible substitutes, each with their advantages and limitations. Stainless steel is a commonly explored alternative due to its lower cost, good mechanical properties, and reasonable corrosion resistance, although it may suffer from passivation or corrosion under certain electrochemical oxidation conditions. Ni substrates are another option, offering good conductivity and durability in alkaline environments; however, they are prone to corrosion in acidic conditions. Ta and Nb show excellent corrosion resistance comparable to Ti but remain costly, limiting their widespread use. Al, while inexpensive and lightweight, tends to form non-conductive oxide layers that hinder its performance in electrochemical applications. Each of these alternatives involves trade-offs in cost, durability, and compatibility with specific electrochemical reactions, necessitating careful selection based on the operating environment and performance requirements. While these alternatives present cost advantages, the superior stability, corrosion resistance, excellent conductivity, and durability of Ti substrates often outweigh their higher cost, making titanium a preferred choice for long-term performance in demanding electrochemical applications.

To further advance the development of durable and efficient electrocatalysts, it is crucial to address the gaps in standardization. Stability data of DSA anodes have been obtained under a wide range of test conditions—including different current densities, electrode surface areas, electrolytes, catalyst loadings, and test temperatures—as well as using diverse experimental setups and test techniques (Table 1). This lack of standardization makes it difficult to draw meaningful comparisons regarding the stability of these DSA catalysts. For example, although the RDE technique is frequently used to investigate electrocatalyst stability, the conclusions drawn from these tests often cannot be directly applied to MEA electrolyzer[25, 50–52]. Typically, galvanostatic RDE stability tests result in catalyst lifetimes of only several hours. In contrast, the same catalysts can last for thousands of hours in a MEA electrolyzer under similar conditions—a discrepancy that remains unresolved[25, 51, 52]. This deficiency complicates the accurate comparison of stability across different electrocatalysts. The discrepancy in catalyst lifetimes between RDE tests and MEA electrolyzers arises from differences in mass transport, electrode structure, and operating conditions. RDE tests suffer from limited mass transport, bubble accumulation, and harsh liquid electrolytes, which accelerate catalyst degradation. In contrast, MEA electrolyzers benefit from efficient reactant access, bubble removal, and a controlled membrane environment, leading to significantly longer catalyst lifetimes. Accelerated stress tests, often employed to predict catalyst longevity, do not always accurately mirror real-world operational conditions. These tests accelerate the aging process by exposing electrocatalysts to extreme conditions, but translating these results to predict actual performance under normal working conditions remains challenging. Consequently, developing a reliable and universally accepted framework for stability assessment is crucial to advance not only the field of electrocatalysis but also the practical deployment of these technologies in industrial applications.

Conclusions

In summary, the development of DSA represents a significant technological advancement in the chlor-alkali industry, markedly enhancing the efficiency and stability of chlorine production. By replacing carbon anodes with DSA, the industry achieved substantial reductions in electricity consumption and enhanced the durability of electrochemical systems. The primary advantage of DSAs lies in their improved gas-bubble management, which minimizes mass transport limitations and reduces voltage requirements. This advancement underscores the critical role of both electrocatalyst activity and stability in developing effective industrial catalysts. Furthermore, it highlights the importance of addressing the gas-bubble effect in electrochemical processes, which can significantly impact the stability and efficiency of processes involving gas evolution. These insights can guide future developments in electrochemical technologies and renewable energy applications, emphasizing a holistic approach that focuses on stability, efficiency, and systematic optimization.

References

[1] O'Brien, T. F.; Bommaraju, T. V.; Hine, F. *Handbook of Chlor-Alkali Technology*; Springer: New York, 2005.

[2] Brinkmann, T.; Santonja, G. G.; Schorcht, F.; Roudier, S.; Sancho, L. D. *Best Available Techniques* (*BAT*) *Reference Document for the Production of Chlor-alkali*; Publications Office of the European Union: Luxembourg, 2014.

[3] Li, K.; Fan, Q.; Chuai, H.; Liu, H.; Zhang, S.; Ma, X. B. Revisiting chlor-alkali electrolyzers: From materials to devices. *Trans. Tianjin Univ.* **2021**, *27*, 202–216.

[4] Zeradjanin, A. R. The era of stable electrocatalysis. *Nat. Catal.* **2023**, *6*, 458–459.

[5] Deng, Z. L.; Xu, S. Y.; Liu, C. H.; Zhang, X. Q.; Li, M. F.; Zhao, Z. P. Stability of dimensionally stable anode for chlorine evolution reaction. *Nano Res.* **2024**, *17*, 949–959.

[6] Beer, H. B. The invention and industrial development of metal anodes. *J. Electrochem. Soc.* **1980**, *127*, 303C–307C.

[7] Beer, H. B. Dimensionally stable anodes. In *Electrochemistry in Industry: New Directions*. Landau, U.; Yeager, E.; Kortan, D., Eds.; Springer: New York, 1982; pp 19–28.

[8] Wu, H.; Huang, Q. X.; Shi, Y. Y.; Chang, J. W.; Lu, S. Y. Electrocatalytic water splitting: Mechanism and electrocatalyst design. *Nano Res.* **2023**, *16*, 9142–9157.

[9] Zhai, Y. J.; Han, P.; Yun, Q. B.; Ge, Y. Y.; Zhang, X.; Chen, Y.; Zhang, H. Phase engineering of metal nanocatalysts for electrochemical CO_2 reduction. *eScience* **2022**, *2*, 467–485.

[10] Fu, X. B.; Pedersen, J. B.; Zhou, Y. Y.; Saccoccio, M.; Li, S. F.; Sažinas, R.; Li, K.; Andersen, S. Z.; Xu, A. N.; Deissler, N. H. et al. Continuous-flow electrosynthesis of ammonia by nitrogen reduction and hydrogen oxidation. *Science* **2023**, *379*, 707–712.

[11] Beer, H. B. Inventor a method of chemically plating base layers with precious metals. United Kingdom Patent GB964913A, **1961**.

[12] Beer, H. B. Inventor improvements in or relating to the manufacture of electrodes. United Kingdom Patent GB1195871A, **1967**.

[13] Beer, H. B. Inventor electrode and coating therefor. United States Patent US3632498A, **1972**.

[14] Trasatti, S. Electrocatalysis: Understanding the success of DSA®. *Electrochim. Acta* **2000**, *45*, 2377–2385.

[15] Trasatti, S.; Buzzanca, G. Ruthenium dioxide: A new interesting electrode material. Solid state structure and electrochemical behaviour. *J. Electroanal. Chem. Interfacial Electrochem.* **1971**, *29*, A1–A5.

[16] De Nora, I. O. Anwendung maßbeständiger aktivierter Titan-Anoden bei der chloralkali-elektrolyse. *Chem. Ing. Tech.* **1970**, *42*, 222–226.

[17] Yin, W. N.; Cai, Y. T.; Xie, L. B.; Huang, H.; Zhu, E. C.; Pan, J. A.; Bu, J. Q.; Chen, H.; Yuan, Y.; Zhuang, Z. C. et al. Revisited electrochemical gas evolution reactions from the perspective of gas bubbles. *Nano Res.* **2023**, *16*, 4381–4398.

[18] Zhao, X.; Ren, H.; Luo, L. Gas bubbles in electrochemical gas evolution reactions. *Langmuir* **2019**, *35*, 5392–5408.

[19] Angulo, A.; van der Linde, P.; Gardeniers, H.; Modestino, M.; Rivas, D. F. Influence of bubbles on the energy conversion efficiency of electrochemical reactors. *Joule* **2020**, *4*, 555–579.
[20] Xu, W. W.; Lu, Z. Y.; Sun, X. M.; Jiang, L.; Duan, X. Superwetting electrodes for gas-involving electrocatalysis. *Acc. Chem. Res.* **2018**, *51*, 1590–1598.
[21] Kempler, P. A.; Coridan, R. H.; Luo, L. Gas evolution in water electrolysis. *Chem. Rev.* **2024**, *124*, 10964–11007.
[22] Iwata, R.; Zhang, L. N.; Wilke, K. L.; Gong, S.; He, M. F.; Gallant, B. M.; Wang, E. N. Bubble growth and departure modes on wettable/non-wettable porous foams in alkaline water splitting. *Joule* **2021**, *5*, 887–900.
[23] Park, S.; Liu, L. H.; Demirkır, Ç.; van der Heijden, O.; Lohse, D.; Krug, D.; Koper, M. T. M. Solutal marangoni effect determines bubble dynamics during electrocatalytic hydrogen evolution. *Nat. Chem.* **2023**, *15*, 1532–1540.
[24] Kamat, G. A.; Stevens, M. B. Electrolyte type affects electrochemical bubble formation. *Nat. Chem.* **2023**, *15*, 1488–1489.
[25] Ehelebe, K.; Escalera-López, D.; Cherevko, S. Limitations of aqueous model systems in the stability assessment of electrocatalysts for oxygen reactions in fuel cell and electrolyzers. *Curr. Opin. Electrochem.* **2021**, *29*, 100832.
[26] Wei, C.; Wang, Z. B.; Otani, K.; Hochfilzer, D.; Zhang, K.; Nielsen, R.; Chorkendorff, I.; Kibsgaard, J. Benchmarking electrocatalyst stability for acidic oxygen evolution reaction: The crucial role of dissolved ion concentration. *ACS Catal.* **2023**, *13*, 14058–14069.
[27] Loučka, T. The reason for the loss of activity of titanium anodes coated with a layer of RuO_2 and TiO_2. *J. Appl. Electrochem.* **1977**, *7*, 211–214.
[28] Hine, F.; Yasuda, M.; Noda, T.; Yoshida, T.; Okuda, J. Electrochemical behavior of the oxide-coated metal anodes. *J. Electrochem. Soc.* **1979**, *126*, 1439–1445.
[29] Yeo, R. S.; Orehotsky, J.; Visscher, W.; Srinivasan, S. Ruthenium-based mixed oxides as electrocatalysts for oxygen evolution in acid electrolytes. *J. Electrochem. Soc.* **1981**, *128*, 1900–1904.
[30] Scarpellino, A. J.; Fisher, G. L. The development of an energy-efficient insoluble anode for nickel electrowinning: II. Multilayer precious metal coatings. *J. Electrochem. Soc.* **1982**, *129*, 522–525.
[31] Comninellis, C.; Vercesi, G. P. Characterization of DSA®-type oxygen evolving electrodes: Choice of a coating. *J. Appl. Electrochem.* **1991**, *21*, 335–345.
[32] Mráz, R.; Krýsa, J. Long service life IrO_2/Ta_2O_5 electrodes for electroflotation. *J. Appl. Electrochem.* **1994**, *24*, 1262–1266.
[33] De Faria, L. A.; Boodts, J. F. C.; Trasatti, S. Electrocatalytic properties of ternary oxide mixtures of composition $Ru_{0.3}Ti_{0.7-x}Ce_xO_2$: Oxygen evolution from acidic solution. *J. Appl. Electrochem.* **1996**, *26*, 1195–1199.
[34] Correa-Lozano, B.; Comninellis, C.; De Battisti, A. Service life of Ti/SnO_2-Sb_2O_5 anodes. *J. Appl. Electrochem.* **1997**, *27*, 970–974.
[35] Alves, V. A.; Da Silva, L. A.; Boodts, J. F. C. Electrochemical impedance spectroscopic study of dimensionally stable anode corrosion. *J. Appl. Electrochem.* **1998**, *28*, 899–905.
[36] Terezo, A. J.; Pereira, E. C. Fractional factorial design applied to investigate properties of Ti/IrO_2-Nb_2O_5 electrodes. *Electrochim. Acta* **2000**, *45*, 4351–4358.
[37] Chen, X. M.; Chen, G. H.; Yue, P. L. Stable Ti/IrO_x-Sb_2O_5-SnO_2 anode for O_2 evolution with low Ir content. *J. Phys. Chem. B* **2001**, *105*, 4623–4628.
[38] Hu, J. M.; Meng, H. M.; Zhang, J. Q.; Cao, C. N. Degradation mechanism of long service life Ti/IrO_2-Ta_2O_5 oxide anodes in sulphuric acid. *Corros. Sci.* **2002**, *44*, 1655–1668.
[39] Fernández, J. L.; De Chialvo, M. R. G.; Chialvo, A. C. Preparation and electrochemical characterization of $Ti/Ru_xMn_{1-x}O_2$ electrodes. *J. Appl. Electrochem.* **2002**, *32*, 513–520.
[40] Xu, L. K.; Scantlebury, J. D. A study on the deactivation of an IrO_2-Ta_2O_5 coated titanium anode. *Corros. Sci.* **2003**, *45*, 2729–2740.
[41] Chen, X. M.; Chen, G. H. Stable Ti/RuO_2-Sb_2O_5-SnO_2 electrodes for O_2 evolution. *Electrochim Acta* **2005**, *50*, 4155–4159.
[42] Li, B. S.; Lin, A.; Gan, F. X. Preparation and electrocatalytic properties of Ti/IrO_2-Ta_2O_5 anodes for oxygen evolution. *Trans. Nonferrous Met. Soc. China* **2006**, *16*, 1193–1199.
[43] Hoseinieh, S. M.; Ashrafizadeh, F.; Maddahi, M. H. A comparative investigation of the corrosion behavior of RuO_2-IrO_2-TiO_2 coated titanium anodes in chloride solutions. *J. Electrochem. Soc.* **2010**, *157*, E50–E56.
[44] Chen, S. Y.; Zheng, Y. H.; Wang, S. W.; Chen, X. M. Ti/RuO_2-Sb_2O_5-SnO_2 electrodes for chlorine evolution from seawater. *Chem. Eng. J.* **2011**, *172*, 47–51.
[45] Fathollahi, F.; Javanbakht, M.; Norouzi, P.; Ganjali, M. R. Comparison of morphology, stability and electrocatalytic properties of $Ru_{0.3}Ti_{0.7}O_2$ and $Ru_{0.3}Ti_{0.4}Ir_{0.3}O_2$ coated titanium anodes. *Russ. J. Electrochem.* **2011**, *47*, 1281–1286.
[46] Wang, S. W.; Xu, H. L.; Yao, P. D.; Chen, X. M. Ti/RuO_2-IrO_2-SnO_2-Sb_2O_5 anodes for Cl_2 evolution from seawater. *Electrochemistry* **2012**, *80*, 507–511.
[47] Hoseinieh, S. M.; Ashrafizadeh, F. Influence of electrolyte composition on deactivation mechanism of a $Ti/Ru_{0.25}Ir_{0.25}Ti_{0.5}O_2$ electrode. *Ionics* **2013**, *19*, 113–125.
[48] Yan, Z. W.; Zhao, Y. W.; Zhang, Z. Z.; Li, G.; Li, H. C.; Wang, J. S.; Feng, Z. Q.; Tang, M. Q.; Yuan, X. J.; Zhang, R. Z. et al. A study on the performance of IrO_2-Ta_2O_5 coated anodes with surface treated Ti substrates. *Electrochim. Acta* **2015**, *157*, 345–350.
[49] Zheng, Y. R.; Vernieres, J.; Wang, Z. B.; Zhang, K.; Hochfilzer, D.; Krempl, K.; Liao, T. W.; Presel, F.; Altantzis, T.; Fatermans, J. et al. Monitoring oxygen production on mass-selected iridium-tantalum oxide electrocatalysts. *Nat. Energy* **2022**, *7*, 55–64.
[50] Zlatar, M.; Escalera-López, D.; Rodríguez, M. G.; Hrbek, T.; Götz, C.; Joy, R. M.; Savan, A.; Tran, H. P.; Nong, H. N.; Pobedinskas, P. et al. Standardizing OER electrocatalyst benchmarking in aqueous electrolytes: Comprehensive guidelines for accelerated stress tests and backing electrodes. *ACS Catal.* **2023**, *13*, 15375–15392.
[51] El-Sayed, H. A.; Weiß, A.; Olbrich, L. F.; Putro, G. P.; Gasteiger, H. A. OER catalyst stability investigation using RDE technique: A stability measure or an artifact. *J. Electrochem. Soc.* **2019**, *166*, F458–F464.
[52] Tovini, M. F.; Hartig-Weiß, A.; Gasteiger, H. A.; El-Sayed, H. A. The discrepancy in oxygen evolution reaction catalyst lifetime explained: RDE vs MEA-dynamicity within the catalyst layer matters. *J. Electrochem. Soc.* **2021**, *168*, 014512.

Data availability

Not applicable.

Acknowledgements

X.F. was supported under the MSCA European Postdoctoral Fellowships (Electro-Ammonia Project 101059643).

Author contributions

X.F.: Conceptualization, supervision, investigation, visualization, writing of original draft, review, and editing.

Competing interests

The author declare that he has no competing interests.